

Vehicle Models and Optimal Control on a Nonplanar Surface

Thomas Fork¹, H. Eric Tseng², and Francesco Borrelli¹

¹UC Berkeley, ²Ford Research & Advanced Engineering

Email: fork@berkeley.edu

We present a 10 DoF dynamic vehicle model for model-based control on nonplanar road surfaces. A parametric surface is used to describe the road surface, allowing the surface parameterization to describe the pose of the vehicle. We use the proposed approach to compute minimum-time vehicle trajectories on nonplanar surfaces and compare planar and nonplanar models.

Topics: Vehicle Dynamics Theory, Modeling

1. BACKGROUND

Model-based motion planning and control is widely used for vehicles [1]. However, commonly used models are limited to flat surfaces, limiting applicability of related control techniques. In [2] we developed an approach for modeling vehicles on arbitrary nonplanar surfaces and focused on kinematic models. In this paper we leverage our approach to develop a 10 DoF dynamic vehicle model for nonplanar model-based control and use our model to compute minimum time trajectories on nonplanar surfaces.

The contributions of this paper are:

1. We develop a nonplanar dynamic vehicle model which includes tire forces and dynamic weight distribution.
2. We use our dynamic vehicle model for optimal control on a nonplanar road surface.
3. We compare our model to other nonplanar and planar vehicle models.

This paper is structured as follows: In sections 2 and 3 we introduce our vehicle model. We then use this model for optimal control in section 4. We present results and conclusions in sections 5 and 6.

2. NONPLANAR VEHICLE MODELING

We use the frames of reference, variables and modeling approach of [2]*: we model a vehicle as a rigid body in tangent contact with a parametric surface and use the surface parameterization to describe the pose of the vehicle. This requires several key assumptions:

- The vehicle is treated as a single rigid body
- This body remains tangent to the road as it moves
- Contact with the road is never lost
- Out of plane road curvature is small relative to the length of the vehicle

We develop our model in five steps:

1. We describe the road with a parametric surface
2. We relate vehicle velocity to motion on this surface

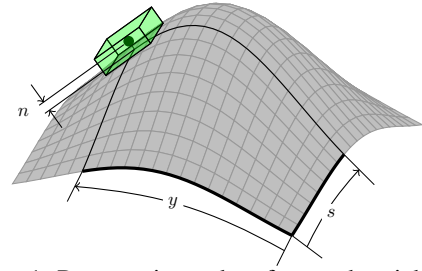


Fig. 1: Parametric road surface and variables

3. Rigid body equations of motion are introduced
4. Tire forces and other forces are introduced
5. Weight distribution effects are added

These steps are elaborated in the following subsections.

2.1. Parametric Road Surface

We describe the road surface with a known parametric surface $\mathbf{x}^p(s, y)$ where \mathbf{x}^p is a vector in \mathbb{R}^3 in an inertial frame of reference and s and y are parameterization variables (often, but not necessarily path length and lane offset respectively). We assume that this road surface is smooth, time invariant and regular, meaning that the tangent vectors of the surface are linearly independent. We extend [2] in adding a third parametric variable: n , to offset the vehicle center of mass (COM) normal to the parametric surface**. This is illustrated in Figure 1.

We denote the tangent vectors with the partial derivatives $\frac{\partial}{\partial s}\mathbf{x}^p = \mathbf{x}_s^p$ and $\frac{\partial}{\partial y}\mathbf{x}^p = \mathbf{x}_y^p$. We define the outward normal vector \mathbf{e}_n^p as

$$\mathbf{e}_n^p = \frac{\mathbf{x}_s^p \times \mathbf{x}_y^p}{\|\mathbf{x}_s^p \times \mathbf{x}_y^p\|}. \quad (1)$$

Variables s and y describe position on the surface; to describe orientation we introduce θ^s as shown in Figure 2, with the mathematical definition below:

$$\cos(\theta^s) = \frac{\mathbf{e}_1^b \cdot \mathbf{x}_s^p}{\|\mathbf{x}_s^p\|} \quad (2a)$$

**Without this, in [2], it was necessary to use a parametric surface that always contained the center of mass of the vehicle: an offset of the true road surface.

A video can be found at <https://youtu.be/4nCYGIKpd2A>

Source code:

<https://github.com/thomasfork/Nonplanar-Vehicle-Control>

*The reader may find it useful to read section II thereof.

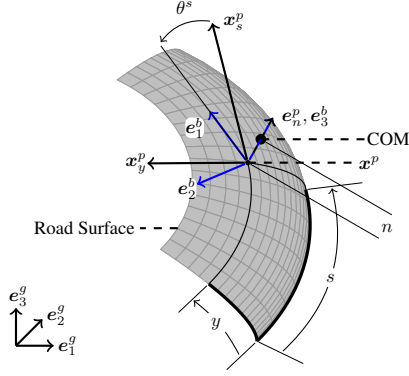


Fig. 2: Coordinate systems and θ^s

$$\sin(\theta^s) = \frac{-\mathbf{e}_2^b \cdot \mathbf{x}_s^p}{\|\mathbf{x}_s^p\|}. \quad (2b)$$

Imposing tangent contact means imposing the constraints

$$\mathbf{x}^p + n\mathbf{e}_n^p = \mathbf{x}^g \quad (3a)$$

$$\mathbf{e}_3^b \cdot \mathbf{x}_s^p = 0 \quad (3b)$$

$$\mathbf{e}_3^b \cdot \mathbf{x}_y^p = 0. \quad (3c)$$

where \mathbf{x}^g is position in the global, inertial frame of reference.

2.2. Parametric Motion Equations

We first relate linear and angular velocity of the vehicle in the body frame to the time derivative of vehicle pose: \dot{s} , \dot{y} , \dot{n} and $\dot{\theta}^s$, providing the first set of equations for our vehicle model. As in [2], we do so by differentiating constraints (2) and (3) with respect to time. Only (3a) has changed, so we reuse the results of [2] for the remaining equations:

$$\underbrace{\begin{bmatrix} \mathbf{x}_{ss}^p \cdot \mathbf{e}_n^p & \mathbf{x}_{sy}^p \cdot \mathbf{e}_n^p \\ \mathbf{x}_{ys}^p \cdot \mathbf{e}_n^p & \mathbf{x}_{yy}^p \cdot \mathbf{e}_n^p \end{bmatrix}}_{\mathbf{II}} \begin{bmatrix} \dot{s} \\ \dot{y} \end{bmatrix} = \underbrace{\begin{bmatrix} \mathbf{x}_s^p \cdot \mathbf{e}_1^b & \mathbf{x}_s^p \cdot \mathbf{e}_2^b \\ \mathbf{x}_y^p \cdot \mathbf{e}_1^b & \mathbf{x}_y^p \cdot \mathbf{e}_2^b \end{bmatrix}}_{\mathbf{J}} \begin{bmatrix} -\omega_2^b \\ \omega_1^b \end{bmatrix} \quad (4)$$

$$\begin{aligned} \dot{\theta}^s = \omega_3^b + & \frac{(\mathbf{x}_{ss}^p \times \mathbf{x}_s^p) \cdot \mathbf{e}_n^p}{\mathbf{x}_s^p \cdot \mathbf{x}_s^p} \dot{s} \\ & + \frac{(\mathbf{x}_{sy}^p \times \mathbf{x}_y^p) \cdot \mathbf{e}_n^p}{\mathbf{x}_s^p \cdot \mathbf{x}_s^p} \dot{y}. \end{aligned} \quad (5)$$

\mathbf{x}_{ss}^p is our notation for a second partial derivative. Recognizing that $\frac{d}{dt}\mathbf{e}_n^p = \frac{d}{dt}\mathbf{e}_3^b = \omega_2^b\mathbf{e}_1^b - \omega_1^b\mathbf{e}_2^b$, the time derivative of (3a) is:

$$\begin{aligned} \dot{s}\mathbf{x}_s^p + \dot{y}\mathbf{x}_y^p + \dot{n}\mathbf{e}_n^p + n(\omega_2^b\mathbf{e}_1^b - \omega_1^b\mathbf{e}_2^b) \\ = v_1^b\mathbf{e}_1^b + v_2^b\mathbf{e}_2^b + v_3^b\mathbf{e}_3^b \end{aligned} \quad (6)$$

which we simplify by taking inner products with respect to \mathbf{x}_s^p , \mathbf{x}_y^p and \mathbf{e}_n^p :

$$\begin{aligned} \underbrace{\begin{bmatrix} \mathbf{x}_s^p \cdot \mathbf{e}_1^b & \mathbf{x}_s^p \cdot \mathbf{e}_2^b \\ \mathbf{x}_y^p \cdot \mathbf{e}_1^b & \mathbf{x}_y^p \cdot \mathbf{e}_2^b \end{bmatrix}}_{\mathbf{J}} \left(\begin{bmatrix} v_1^b \\ v_2^b \end{bmatrix} + n \begin{bmatrix} -\omega_2^b \\ \omega_1^b \end{bmatrix} \right) \\ = \underbrace{\begin{bmatrix} \mathbf{x}_s^p \cdot \mathbf{x}_s^p & \mathbf{x}_s^p \cdot \mathbf{x}_y^p \\ \mathbf{x}_y^p \cdot \mathbf{x}_s^p & \mathbf{x}_y^p \cdot \mathbf{x}_y^p \end{bmatrix}}_{\mathbf{I}} \begin{bmatrix} \dot{s} \\ \dot{y} \end{bmatrix} \end{aligned} \quad (7)$$

$$\dot{n} = v_3^b. \quad (8)$$

Using (4) we simplify (7) to:

$$\begin{bmatrix} \dot{s} \\ \dot{y} \end{bmatrix} = (\mathbf{I} - n\mathbf{II})^{-1} \mathbf{J} \begin{bmatrix} v_1^b \\ v_2^b \end{bmatrix} \quad (9)$$

which when $n = 0$ is identical to the expression obtained in [2]. Together, (5), (8) and (9) relate vehicle velocity to parametric velocity $(\dot{s}, \dot{y}, \dot{n}, \dot{\theta}^s)$ and (4) gives the necessary angular velocity ω_1^b and ω_2^b to follow a curved surface while remaining tangent to it.

Note that combining (4) and (9) we get

$$\begin{bmatrix} -\omega_2^b \\ \omega_1^b \end{bmatrix} = \mathbf{J}^{-1}\mathbf{II} (\mathbf{I} - n\mathbf{II})^{-1} \mathbf{J} \begin{bmatrix} v_1^b \\ v_2^b \end{bmatrix} \quad (10)$$

which represents the curvature of the road surface in the body frame of the vehicle.

In the following section $\dot{\omega}_1^b$ and $\dot{\omega}_2^b$ will impact the weight distribution of a vehicle, necessitating expressions for both. Whereas the previous expressions are exact we make the approximation:

$$\begin{bmatrix} -\dot{\omega}_2^b \\ \dot{\omega}_1^b \end{bmatrix} = \mathbf{J}^{-1}\mathbf{II} (\mathbf{I} - n\mathbf{II})^{-1} \mathbf{J} \begin{bmatrix} \dot{v}_1^b \\ \dot{v}_2^b \end{bmatrix}. \quad (11)$$

This assumes that the curvature of the surface changes gradually enough that the omitted terms are negligible. We claim this is the case for road surfaces of interest, as we have already assumed the road curvature is small relative to the length of the vehicle.

Henceforth we limit ourselves to the case $\dot{n} = 0$.

2.3. Vehicle Velocity Equations

We derive velocity equations of motion by simplifying the Newton Euler equations for our modeling approach. We use the common assumption that the moment of inertia matrix of a vehicle is diagonal [3, Ch. 9]. Written out, the equations are [4]:

$$\dot{v}_1^b + v_3^b\omega_2^b - v_2^b\omega_3^b = \frac{1}{m}F_1^b \quad (12a)$$

$$\dot{v}_2^b + v_1^b\omega_3^b - v_3^b\omega_1^b = \frac{1}{m}F_2^b \quad (12b)$$

$$\dot{v}_3^b + v_2^b\omega_1^b - v_1^b\omega_2^b = \frac{1}{m}F_3^b \quad (12c)$$

$$I_1^b\dot{\omega}_1^b + (I_3^b - I_2^b)\omega_2^b\omega_3^b = K_1^b \quad (12d)$$

$$I_2^b\dot{\omega}_2^b + (I_1^b - I_3^b)\omega_3^b\omega_1^b = K_2^b \quad (12e)$$

$$I_3^b\dot{\omega}_3^b + (I_2^b - I_1^b)\omega_1^b\omega_2^b = K_3^b. \quad (12f)$$

Equations (12c), (12d) and (12e) are constrained by our tangent contact assumption and impact weight distribution. We solve the remaining parts of (12) to derive velocity equations of motion. We consider three sources of force \mathbf{F}^b and moment \mathbf{K}^b in (12): gravity $\mathbf{F}^{g,b}$, tire forces and drag $\mathbf{F}^{d,b}$, $\mathbf{K}^{d,b}$. We assume that gravity and drag are functions of the vehicle state, ie. pose and velocity, whereas tire forces must be found by solving for the weight distribution of the vehicle as in [5]. Once we collect the vehicle pose, velocity, tire force and

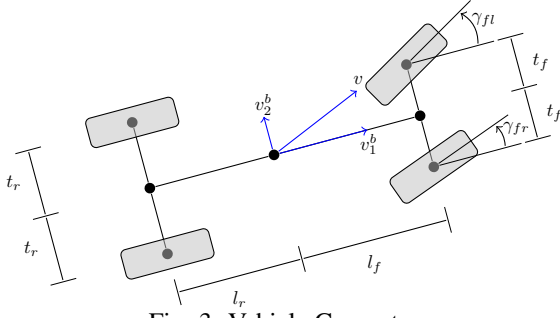


Fig. 3: Vehicle Geometry

input variables, we obtain a differential algebraic model (DAE), which we cast in the semi-explicit form:

$$\dot{\mathcal{Z}} = f(\mathcal{Z}, \mathcal{U}, \mathcal{G}) \quad (13a)$$

$$0 = g_c(\mathcal{Z}, \mathcal{U}, \mathcal{G}) \quad (13b)$$

where \mathcal{Z} is a state vector, \mathcal{U} an input vector and \mathcal{G} a vector of algebraic states. Vehicle dynamics are captured by f with weight distribution enforced by g_c . Next we define \mathcal{Z} , \mathcal{U} and \mathcal{G} for our model and derive f and g_c

2.4. Two Track Vehicle Model

First we define basic vehicle geometry, as shown in Figure 3. We use l_f and l_r for the distance to the front and rear axle from the center of mass respectively. We use t_f for half the width of the front axle and t_r for half the width of the rear axle. We use Ackermann steering for the front steering angles γ_{fr} and γ_{fl} with a single front steering angle input γ . We also treat the slip ratio of each tire as an input. With this in mind, the state and input variables in (13) are:

$$\mathcal{Z} = [s, y, \theta^s, v_1^b, v_2^b, \omega_3^b] \quad (14a)$$

$$\mathcal{U} = [\sigma_{fr}, \sigma_{fl}, \sigma_{rr}, \sigma_{rl}, \gamma] \quad (14b)$$

where σ_{ij} is the slip ratio of a given tire with the first index corresponding to front (f) or rear (r) and the second to right (r) or left (l) side of the vehicle. A simple choice for \mathcal{G} is $\mathcal{G} = [N_{fr}, N_{rl}, N_{rr}, N_{rl}]$, where N_{ij} is the normal force on a given tire. We present a simpler expression for \mathcal{G} in the following section.

We model each tire with a combined slip Pacejka tire model that is linear in normal force and based on [6, pgs. 179-182]. Using the notation of [6] we have:

$$F_x = F_{x0} G_{xa} \quad (15a)$$

$$G_{xa} = \cos(C_{xa} \arctan(B_{xa} \alpha - E_{xa}(B_{xa} \alpha - \arctan(B_{xa} \alpha)))) \quad (15b)$$

$$B_{xa} = r_{Bx1} \cos(\arctan(r_{Bx2} \sigma)) \quad (15c)$$

$$F_{x0} = \mu N \sin(C_x \arctan(B_x \sigma - E_x(B_x \sigma - \arctan(B_x \sigma)))) \quad (15d)$$

$$F_y = F_{y0} G_{ys} \quad (15e)$$

$$G_{ys} = \cos(C_{ys} \arctan(B_{ys} \sigma - E_{ys}(B_{ys} \sigma - \arctan(B_{ys} \sigma)))) \quad (15f)$$

$$B_{ys} = r_{By1} \cos(\arctan(r_{By2} \alpha)) \quad (15g)$$

$$F_{y0} = \mu N \sin(C_y \arctan(B_y \alpha - E_y(B_y \alpha - \arctan(B_y \alpha)))) \quad (15h)$$

where σ and α are the slip ratio and slip angle of the tire and N the normal force on the tire. Parameters are provided in Table 3 at the end of this paper. F_x and F_y are the lateral and longitudinal forces on the tire. We express this in the body frame in the form:

$$F_{ij,1}^{t,b} = N_{ij} \mu_{ij,1}(\sigma_{ij}, \alpha_{ij}, \gamma_{ij}) \quad (16a)$$

$$F_{ij,2}^{t,b} = N_{ij} \mu_{ij,2}(\sigma_{ij}, \alpha_{ij}, \gamma_{ij}) \quad (16b)$$

where ij refers to any given tire and $\mu_{ij,1}$ and $\mu_{ij,2}$ capture remaining tire model terms, which are functions of \mathcal{Z} and \mathcal{U} .

We follow the slip definitions in [6, pg. 67], whereby the slip angle α is

$$\alpha = \arctan\left(-\frac{V_{cy}}{V_{cx}^*}\right) \quad (17)$$

here V_{cy} is the lateral velocity of the tire at the surface of the road and V_{cx}^* is the longitudinal velocity of the tire at the tire's effective radius. Both follow from translating the linear and angular of the vehicle to the rolling radius r or effective radius r_e of the tire and applying a rotation based on the steering angle of the tire. The expressions for this are straightforward and omitted here. Note that the effect of a curved surface is captured by nonzero ω_1^b and ω_2^b in this translation, a result of Equation (10).

We can now fill in the expressions for the net force and torque on the vehicle:

$$F_1^b = F_1^{d,b} + F_1^{g,b} + F_1^{t,b} \quad (18a)$$

$$F_2^b = F_2^{d,b} + F_2^{g,b} + F_2^{t,b} \quad (18b)$$

$$F_3^b = F_3^{d,b} + F_3^{g,b} + F_3^{t,b} \quad (18c)$$

$$K_1^b = K_1^{d,b} + hF_2^{t,b} - N_{fr}t_f + N_{fl}t_f - N_{rr}t_r + N_{rl}t_r \quad (18d)$$

$$K_2^b = K_2^{d,b} - hF_1^{t,b} - (N_{fr} + N_{fl})l_f + (N_{rr} + N_{rl})l_r \quad (18e)$$

$$K_3^b = K_3^{d,b} + K_3^{t,b} \quad (18f)$$

where $F_1^{t,b} = F_{fr,1}^{t,b} + F_{fl,1}^{t,b} + F_{rr,1}^{t,b} + F_{rl,1}^{t,b}$ and likewise for $F_2^{t,b}$. $K_3^{t,b}$ is the yaw torque produced by all longitudinal and lateral tire forces.

We now have all the expressions necessary to define $f(\mathcal{Z}, \mathcal{U}, \mathcal{G})$ from Equation (13). Section 2.2 filled in the first three terms of $\dot{\mathcal{Z}}$, we can compute longitudinal and lateral tire forces from equations (15a) through (15h), compute the resultant force and torque at the vehicle center of mass, add drag and gravity forces and use those expressions in (12a), (12b) and (12f) along with constraints from Section 2.2. This completes the first half of our DAE model. We obtain $g_c(\mathcal{Z}, \mathcal{U}, \mathcal{G})$ next by enforcing weight distribution constraints on \mathcal{G} .

2.5. Weight Distribution

We extend the approach of [5] to a vehicle on a nonplanar surface and derive the resulting force balance expressions.

This involves four constraints to determine the four normal forces of each tire:

1. Balance of the net normal force on the vehicle to remain in contact with the surface
 2. Longitudinal torque on the vehicle body
 3. Lateral torque on the vehicle body
 4. A compatibility expression such as developed in [5]
- We use the compatibility expression of [5]:

$$N_{fr}t_r - N_{fl}t_r - N_{rr}t_f + N_{rl}t_f = 0. \quad (19)$$

As in [5] we make this constraint implicit by introducing the variables N_f , N_r and Δ for which we have

$$N_{fr} = \frac{1}{2}N_f - t_f\Delta \quad (20a)$$

$$N_{fl} = \frac{1}{2}N_f + t_f\Delta \quad (20b)$$

$$N_{rr} = \frac{1}{2}N_r - t_r\Delta \quad (20c)$$

$$N_{rl} = \frac{1}{2}N_r + t_r\Delta. \quad (20d)$$

As a result, we choose

$$\mathcal{G} = [N_f, N_r, \Delta] \quad (21)$$

for our DAE model (13). It remains to find g_c .

Since our DAE is in semi-explicit form we can find g_c with the following approach:

1. Compute $\dot{\mathcal{Z}}$ using f and a guess for \mathcal{G}
2. Find constraint forces and torques needed by $\dot{\mathcal{Z}}$
3. Use these forces and torques to find a required $\hat{\mathcal{G}}$
4. g_c is then $\hat{\mathcal{G}}(\mathcal{Z}, \mathcal{U}, \mathcal{G}) - \mathcal{G} = 0$

First we compute the required net force on the vehicle using the Newton Euler equations:

$$F_{3,\text{required}}^b = m (\dot{v}_3^b + v_2^b\omega_1^b - v_1^b\omega_2^b) \quad (22a)$$

$$K_{1,\text{required}}^b = I_1^b\dot{\omega}_1^b + (I_3^b - I_2^b)\omega_2^b\omega_3^b \quad (22b)$$

$$K_{2,\text{required}}^b = I_2^b\dot{\omega}_2^b + (I_1^b - I_3^b)\omega_3^b\omega_1^b \quad (22c)$$

where terms not part of \mathcal{Z} can be computed from it (such as ω_1^b) using expressions from Section 2.2.

Next we remove drag forces, gravity forces and longitudinal/lateral tire forces to leave only the contributions of the normal force:

$$F_{3N,\text{required}}^b = F_{3,\text{required}}^b - F_3^{d,b} - F_3^{g,b} \quad (23a)$$

$$K_{1N,\text{required}}^b = K_{1,\text{required}}^b - K_1^{d,b} - hF_2^{t,b} \quad (23b)$$

$$K_{2N,\text{required}}^b = K_{2,\text{required}}^b - K_2^{d,b} + hF_1^{t,b}. \quad (23c)$$

Finally, we impose these constraints to find required N_f , N_r and Δ :

$$N_{f,\text{required}} = \frac{l_r}{L}F_{3N,\text{required}}^b - \frac{1}{L}K_{2N,\text{required}}^b \quad (24a)$$

$$N_{r,\text{required}} = \frac{l_f}{L}F_{3N,\text{required}}^b + \frac{1}{L}K_{2N,\text{required}}^b \quad (24b)$$

$$\Delta_{\text{required}} = \frac{1}{2t_f^2 + 2t_r^2}K_{1N,\text{required}}^b. \quad (24c)$$

This gives us g_c , completing our two track vehicle model.

2.6. Comparison Vehicle Models

We compare the previous model to three others:

First, the kinematic bicycle model of [2] with an added friction cone constraint. We constrain the total acceleration of the vehicle from the tires to be less than $\frac{N\mu}{m}$, where N is the total normal force on the vehicle, found in the same manner as in [2]. Tire forces must balance three forces: the longitudinal acceleration input a , cornering force and the lateral component of gravity, which the tires must oppose to avoid the vehicle slipping sideways. These are combined to form the friction cone constraint.

Second, we compare to a planar kinematic bicycle model - one in which the road surface has been projected to a flat plane, identical to the Frenet frame.

Finally, we use a nonplanar dynamic bicycle model where we treat the longitudinal acceleration as an input but include lateral tire forces. We do so with quasi-static weight distribution: the total normal force is distributed between the front and rear wheels as it would be for a stationary vehicle on a flat surface. We also limit the acceleration input within $\pm \frac{N\mu}{m}$.

3. SURFACE PARAMETERIZATION

Thus far, no specific surface parameterization has been used, only knowledge of \mathbf{x}_s^p and other partial derivatives of the surface. This allows our approach to capture different surfaces and parameterizations seamlessly. We now introduce a specific surface parameterization for use in numerical experiments.

We use and extend the Tait Bryan angle surface introduced in [2]. This is a generalization of the Frenet Frame to arbitrary curvature, wherein the tangent \mathbf{e}_s^c , normal \mathbf{e}_n^c and binormal \mathbf{e}_y^c vectors of a curve in \mathbb{R}^3 are given by three Tait-Bryan angles. A parametric surface is then obtained by integrating the tangent vector to obtain a curve, and applying a linear binormal offset:

$$\frac{d\mathbf{x}^c}{ds} = \mathbf{e}_s^c(s) \quad (25)$$

$$\mathbf{x}^p(s, y) = \mathbf{x}^c(s) + y\mathbf{e}_y^c(s). \quad (26)$$

More details on this may be found in [2]. Note that $\mathbf{e}_n^c \neq \mathbf{e}_n^p$, the latter must be computed from \mathbf{x}_s^p and \mathbf{x}_y^p .

We extend this surface parameterization by adding a normal offset, ie. the cross section of the road is no longer flat. Instead of (26) we use the expression:

$$\mathbf{x}^p(s, y) = \mathbf{x}^c(s) + y\mathbf{e}_y^c(s) + \mathbf{e}_n^c \frac{1}{\kappa} \left(1 - \sqrt{1 - y^2\kappa^2}\right) \quad (27)$$

which for $\kappa \neq 0$ and $|y| \leq \frac{1}{\kappa}$ gives us an arc segment. This is illustrated later in Figure 5.

With this normal offset, the surface parameterization is no longer orthogonal, complicating computation of \mathbf{J} . In [2] we introduced a method to compute \mathbf{J} for orthogonal surface parameterizations using θ^s . Here we introduce

the general method:

$$\theta^p = -\sin^{-1}\left(\frac{\mathbf{x}_s^p \cdot \mathbf{x}_y^p}{\|\mathbf{x}_s^p\| \|\mathbf{x}_y^p\|}\right) \quad (28a)$$

$$\mathbf{J} = \begin{bmatrix} \cos(\theta^s) \|\mathbf{x}_s^p\| & -\sin(\theta^s) \|\mathbf{x}_s^p\| \\ \sin(\theta^s - \theta^p) \|\mathbf{x}_y^p\| & \cos(\theta^s - \theta^p) \|\mathbf{x}_y^p\| \end{bmatrix} \quad (28b)$$

where the only difference from [2] is the added θ^p , which is an angular measure of how far the surface parameterization is from orthogonal.

4. OPTIMAL CONTROL

4.1. Vehicle Models

We use our two track and comparison models to compute minimum time trajectories on nonplanar surfaces. For bicycle models we limit the net normal force on the vehicle:

$$0 \leq N \leq N_{max} \quad (29)$$

and limit individual tire forces for the two track model:

$$0 \leq N_{ij} \leq \frac{1}{2} N_{max} \quad (30)$$

where we use $\frac{1}{2}$ instead of $\frac{1}{4}$ to reflect a need for overconservatism in the simpler models*.

4.2. Optimization Framework

We used collocation [7, ch. 10] to set up a raceline optimization problem using our model. Collocation is widely used for raceline computation [8, 9]; we refer the reader to the previous three references for more information. We used 7th order Gauss-Legendre collocation with 100 intervals of uniform path length along the length of the track. To improve numerical performance we normalized the algebraic state \mathcal{G} by mg . We penalized the lap time of the raceline with quadratic regularization applied to input and input rate: $J = \int (1 + \mathbf{u}^T \mathbf{R} \mathbf{u} + \dot{\mathbf{u}}^T \mathbf{R}_d \dot{\mathbf{u}}) dt$. We used $\mathbf{R} = \mathbf{R}_d = 0.001 \mathbf{I}$, where \mathbf{I} is an appropriately sized identity matrix. For closed tracks we enforced a loop closure constraint on state and input variables, otherwise we fixed the initial state of the vehicle.

5. RESULTS

We implemented all vehicle models, the previously described surface parameterization and the raceline problem symbolically in CasADi [10], which was then solved using IPOPT [11] with the linear solver MUMPS [12]. All programs were run and timed on an AMD Ryzen 5700U CPU at 4.3GHz.

To validate our models relative to one another we compared them on a flat, L-shaped track (Figure 4). All three models produced visually identical racelines and lap times as seen in Figure 4, solve times and the time required to set up the NLP in CasADi are reported in Table 1. We omit the planar kinematic bicycle model as it is identical to the general kinematic bicycle model for this flat surface.

*With the simpler models, all force could be distributed on the front wheels without the model capturing this

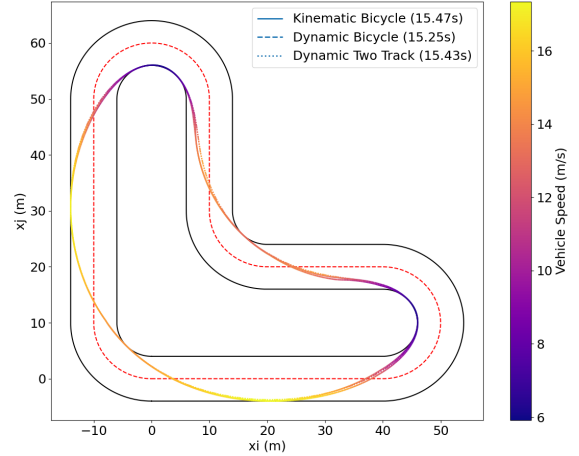


Fig. 4: Planar validation racelines

Table 1: Raceline Solve Times: Planar Track

Time (s)	Kinematic	Dynamic	Two-Track
Setup	3.23	6.14	21.0
IPOPT	0.49	7.07	11.0
NLP Evals	0.14	1.35	7.98

Next we computed racelines on a tube-shaped turn (Figure 5). Here the two track vehicle model achieved a faster lap time than the other two models by leveraging the curved turn to maintain vehicle speed throughout. Racelines are shown in Figure 5 with the color of each car corresponding to the model used. Solve times and the time required to set up the NLP in CasADi for the nonplanar models are reported in Table 2. An animated video of the nonplanar racelines can be found at <https://youtu.be/4nCYGIKpd2A>

6. CONCLUSION

In this paper we developed a two track vehicle model suitable for optimal control on nonplanar surfaces. In contrast to prior work it can be applied systematically to arbitrary nonplanar surfaces and is computationally tractable for model-based control. We demonstrated the use of our model for computing time optimal trajectories on a nonplanar surface, where it outperformed simpler nonplanar vehicle models and a planar vehicle model.

REFERENCES

- [1] B. Paden, M. Čáp, S. Z. Yong, D. Yershov, and E. Frazzoli, “A survey of motion planning and control techniques for self-driving urban vehicles,”

Table 2: Raceline Solve Times: Nonplanar Track

Time (s)	Kinematic		Dynamic	Two-Track
Setup	3.72	10.5	13.3	34.9
IPOPT	1.33	2.21	14.3	37.8
NLP Evals	0.29	1.57	7.41	28.7

The first Kinematic column is the planar model.

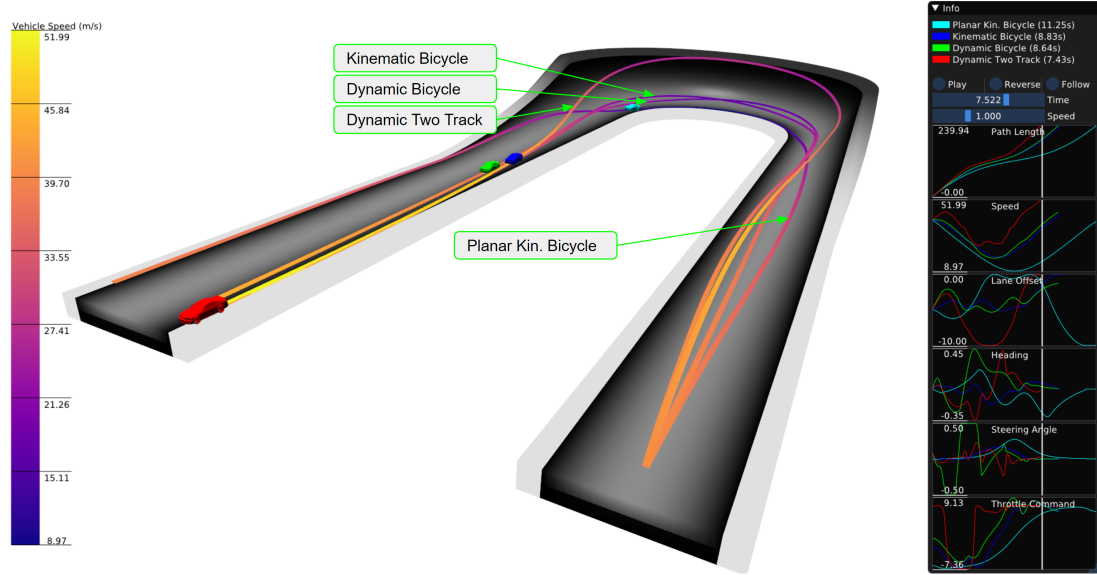


Fig. 5: Nonplanar racelines for each vehicle model. Racelines are colored by speed whereas vehicles are colored by model, with the duration of each raceline in the legend.

- IEEE Transactions on Intelligent Vehicles*, vol. 1, no. 1, pp. 33–55, 2016.
- [2] T. Fork, H. E. Tseng, and F. Borrelli, *Models and predictive control for nonplanar vehicle navigation*, 2021. arXiv: 2104.08427 [eess.SY].
- [3] M. Guiggiani, *The Science of Vehicle Dynamics, Handling, Braking, and Ride of Road and Race Cars*. Springer, 2014.
- [4] L. D. Landau and E. M. Lifshitz, *Mechanics, Course of Theoretical Physics*, 3rd ed. Butterworth-Heinemann, Jan. 1976, vol. 1.
- [5] A. Rucco, G. Notarstefano, and J. Hauser, “Development and numerical validation of a reduced-order two-track car model,” *European Journal of Control*, vol. 20, no. 4, pp. 163–171, 2014.
- [6] H. Pacejka, *Tire and Vehicle Dynamics*, 3rd ed. Butterworth-Heinemann, 2012.
- [7] L. T. Biegler, *Nonlinear Programming, Concepts, Algorithms, and Applications to Chemical Processes*. SIAM, 2010.
- [8] F. Christ, A. Wischnewski, A. Heilmeier, and B. Lohmann, “Time-optimal trajectory planning for a race car considering variable tyre-road friction coefficients,” *Vehicle system dynamics*, vol. 59, no. 4, pp. 588–612, 2021.
- [9] G. Perantoni and D. J. N. Limebeer, “Optimal Control of a Formula One Car on a Three-Dimensional Track—Part 1: Track Modeling and Identification,” *Journal of Dynamic Systems, Measurement, and Control*, vol. 137, no. 5, May 2015.
- [10] J. A. E. Andersson, J. Gillis, G. Horn, J. B. Rawlings, and M. Diehl, “CasADi – A software framework for nonlinear optimization and optimal control,” *Mathematical Programming Computation*, 2018.
- [11] A. Wächter and L. Biegler, “On the implementation of an interior-point filter line-search algorithm for large-scale nonlinear programming,” *Mathematical programming*, vol. 106, pp. 25–57, Mar. 2006.
- [12] P. Amestoy, I. S. Duff, J. Koster, and J.-Y. L’Excellent, “A fully asynchronous multifrontal solver using distributed dynamic scheduling,” *SIAM Journal on Matrix Analysis and Applications*, vol. 23, no. 1, pp. 15–41, 2001.

A. Parameters

Table 3: Vehicle Parameters (MKS where applicable)

Parameter	Value	Parameter	Value
B_x	16	B_y	13
C_x	1.58	C_y	1.45
E_x	0.1	E_y	-0.8
E_{xa}	-0.5	E_{ys}	0.3
C_{xa}	1	C_{ys}	1
r_{Bx1}	13	r_{By1}	10.62
r_{Bx2}	9.7	r_{By2}	7.82
μ	0.75		
r	0.3	r_e	0.3
m	2303	g	9.81
l_f	1.52	l_r	1.50
t_f	0.625	t_r	0.625
h	0.592	I_1^b	956
I_2^b	5000	I_3^b	5520
γ	$\in [-.5, .5]\text{rad}$	N_{max}	40 kN

B. Kinematic Bicycle Friction Cone

As we limit ourselves to tire forces that are linear in normal force, we use a friction cone constraint to enforce that the acceleration magnitude of the bicycle model is less than

$$\frac{\mu N}{m} \quad (31)$$

where once more N is the net normal force on the vehicle.

Three contributions of acceleration are present:

1. The longitudinal acceleration input a
2. Lateral acceleration necessary for cornering
3. Lateral acceleration necessary to avoid sliding on a banked surface

Note that the effect of a sloped surface is captured by altering the expression for \dot{v} , the rate of change of the speed of the vehicle, rather than being part of the tire friction cone constraint.

We model lateral acceleration with the expression

$$\frac{v^2 \gamma}{L} \quad (32)$$

where γ is the front wheel steering angle, L the wheelbase length and their ratio approximates the curvature of the trajectory of the vehicle.

Meanwhile the lateral acceleration necessary on a banked surface is the component of gravity orthogonal to the direction the vehicle is moving. The components of gravity can be found from 3D vehicle orientation, which we derive expressions for in Appendix C. By definition, a kinematic bicycle moves in direction $e_1^b \cos \beta + e_2^b \sin \beta$. With our choices of sign convention, the cornering acceleration to oppose gravity is:

$$a_t^g = -mg (e_1^b \cdot e_3^g \sin \beta - e_2^b \cdot e_3^g \cos \beta) \quad (33)$$

our friction cone constraint is then

$$\left(\frac{m}{\mu N} \right)^2 \left(a^2 + \left(a_t^g + \frac{v^2 \gamma}{L} \right)^2 \right) \leq 1 \quad (34)$$

where we have replaced the Euclidean magnitude with its square for numerical performance benefits, and divided by the squared allowable acceleration to achieve a constraint with constant bound.

C. Computing Vehicle Orientation

Though we describe vehicle pose with the single variable θ^s , it is possible to compute the full 3D pose of the vehicle and to do so from only θ^s and the properties of the parametric surface. Besides being useful for visualization purposes, this is essential to compute gravity components for vehicle models. Furthermore, without describing orientation using only θ^s , we would need full 3D orientation, a rotation matrix, to be a decision variable in model-based control. Here we introduce the general method to compute 3D orientation from θ^s by computing e_1^b , e_2^b and e_3^b from θ^s and first derivatives of the parametric surface.

First, and trivially, we have $e_3^b = x_n^p$, otherwise the vehicle would not be tangent to the surface.

Second we consider the expression:

$$e_1^b = \alpha x_s^p + \beta x_y^p \quad (35a)$$

$$e_2^b = \gamma x_s^p + \delta x_y^p \quad (35b)$$

where α , β , γ and δ are unknowns to solve for. We first split each equation into two equations by taking inner products with respect to x_s^p and x_y^p :

$$\begin{bmatrix} e_1^b \cdot x_s^p \\ e_1^b \cdot x_y^p \end{bmatrix} = \mathbf{I} \begin{bmatrix} \alpha \\ \beta \end{bmatrix} \quad (36a)$$

$$\begin{bmatrix} e_2^b \cdot x_s^p \\ e_2^b \cdot x_y^p \end{bmatrix} = \mathbf{I} \begin{bmatrix} \gamma \\ \delta \end{bmatrix}. \quad (36b)$$

We can merge and solve the two equations by recognizing that they are the columns of \mathbf{J} :

$$\begin{bmatrix} \alpha & \gamma \\ \beta & \delta \end{bmatrix} = \mathbf{I}^{-1} \mathbf{J} \quad (37)$$

Therefore we have (vector symbols treated as column vectors):

$$\begin{bmatrix} e_1^b & e_2^b \end{bmatrix} = \begin{bmatrix} x_s^p & x_y^p \end{bmatrix} \mathbf{I}^{-1} \mathbf{J} \quad (38)$$

which we can compute knowing only θ^s and first order knowledge of the parametric surface.